

GCH 6104 – Rhéologie des polymères

Chapitre 8 Systèmes multiphasés



1

Multiphase systems

- Suspensions → solid particles in a fluid
- Emulsions → liquid droplets in a fluid
- Foams → gas bubbles in a fluid (eventually solid)
- Filled polymer systems
- **Viscosity or resistance to deformation: dispersed and continuous phases move and deform relative to each other**

2

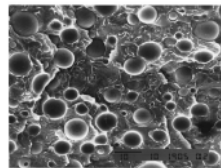
Systems of industrial interest

- Foodstuffs
- Pharmaceutical products
- Paints
- Greases:
 - Emulsions of liquid droplets
 - Suspensions of liquid particles
- Slurries:
 - Mineral and paper pulps
 - Fermentation broths
 - Biological fluids (ex. blood)

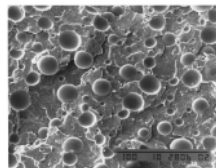
3

Polymer multiphase systems

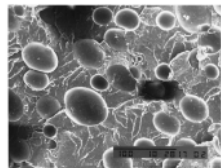
- Short fiber reinforced thermoplastics
- Particles filled polymers
- Polymer blends → immiscible systems



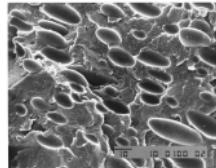
a) $\gamma = 0$



b) $\gamma = 10, \sigma_0 = 25 \text{ Pa}$

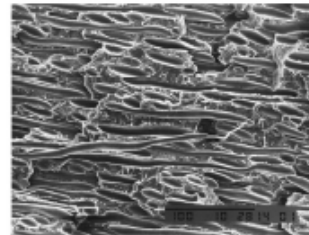


c) $\gamma = 34.5, \sigma_0 = 25 \text{ Pa}$



d) $\gamma = 25, \sigma_0 = 200 \text{ Pa}$

20% HDPE + 80% wt PS
(Martin et al., 2000)



e) $\gamma = 2.35, \sigma_0 = 200 \text{ Pa}$

4

Concentrated suspensions

- Complications under flow conditions:
 - Interface
 - Time variations during processing
 - Orientation of solid particles
 - Agglomeration
 - Breakage
 - Coalescence

5

8.2 Rheology of suspensions

- Rigorous analytical solutions for:
 - Very dilute suspensions of rigid spheres (Einstein, 1906, 1911)
 - Slightly deformable spheres (Taylor, 1932)
 - Ellipsoids (Jeffery, 1922)
- Newtonian media → not of wide practical use
- Theories empirically extended to concentrated systems

6

Einstein relation (1906, 1911)

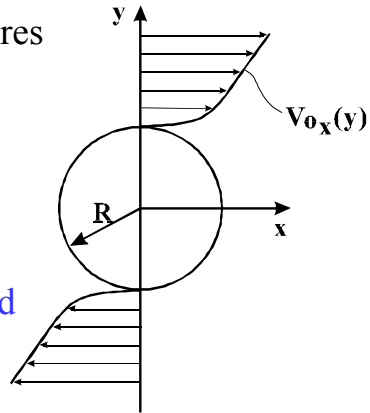
- Very dilute suspensions of rigid spheres
- Low interaction between spheres

$$\mu_r = \frac{\mu_s}{\mu_m} = 1 + \frac{5}{2}\phi$$

μ_s : viscosity of suspension

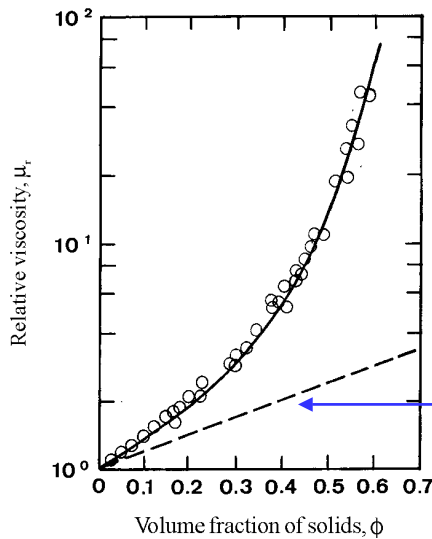
μ_m : viscosity of suspending fluid

ϕ : volume fraction of solids



7

Einstein relation



Suspensions of spheres of low interaction, narrow-size distribution, particle diameters in the range of 0.1 to 440 μm (Thomas 1965)

$$\mu_r = \frac{\mu_s}{\mu_m} = 1 + \frac{5}{2}\phi$$

8

Rheology of emulsions

- Einstein relation adapted by Taylor (1932) for slightly deformable particles
- Dilute emulsion of Newtonian droplets (μ_d) in another Newtonian fluid (μ_m):

$$\mu_r = \frac{\mu_s}{\mu_m} = 1 + \frac{5k + 2}{2k + 2} \phi$$

with $k = \mu_d/\mu_m$

9

Interfacial tension effect

- Interfacial tension α can be accounted for
- Stress tensor in simple shear flow (Schowalter, 1978):

$$\begin{pmatrix} \sigma_{11} & \sigma_{12} & 0 \\ \sigma_{21} & \sigma_{22} & 0 \\ 0 & 0 & \sigma_{33} \end{pmatrix} = - \left[1 + \frac{5k + 2}{2k + 2} \phi \right] \mu_m \begin{pmatrix} 0 & \dot{\gamma} & 0 \\ \dot{\gamma} & 0 & 0 \\ 0 & 0 & 0 \end{pmatrix} - \frac{\mu_m^2 d_p \phi}{2\alpha} \left[\frac{19k + 16}{20(k + 1)^2} \right]$$

$$\left\{ \left[\frac{25k^2 + 41k + 4}{28(k + 1)} \right] \begin{pmatrix} \dot{\gamma}^2 & 0 & 0 \\ 0 & \dot{\gamma}^2 & 0 \\ 0 & 0 & -2\dot{\gamma}^2 \end{pmatrix} - \frac{(19k + 16)}{4} \begin{pmatrix} -\dot{\gamma}^2 & 0 & 0 \\ 0 & \dot{\gamma}^2 & 0 \\ 0 & 0 & 0 \end{pmatrix} \right\}$$

- Elastic properties predicted for emulsions of Newtonian droplets in a Newtonian matrix

10

Gas bubbles

- $k \rightarrow 0$
$$\mu_r = \frac{\mu_s}{\mu_m} = 1 + \varphi$$

- Tiny gas bubbles increase the viscosity of a liquid
- First and second normal stress coefficients become:

$$\psi_1 = -\frac{(\sigma_{11} - \sigma_{22})}{\dot{\gamma}^2} = \frac{32}{10} \frac{\mu_m^2 d_p \phi}{\alpha}$$
$$\psi_2 = -\frac{(\sigma_{22} - \sigma_{33})}{\dot{\gamma}^2} = -\frac{10}{7} \frac{\mu_m^2 d_p \phi}{\alpha}$$

11

Highly viscous droplets

- $k \rightarrow \infty$
$$\psi_1 = \frac{361}{80} \frac{\mu_m^2 d_p \phi}{\alpha}$$
$$\psi_2 = -\frac{551}{560} \frac{\mu_m^2 d_p \phi}{\alpha}$$

- Viscoelastic properties are function of d_p/α (deformability of the droplets)
- Results for the two extreme are very similar \rightarrow unrealistic
- Problem with the assumption of slight deformation of low viscosity droplets at high shear rate

12

Oldroyd's emulsion model (1953,1955)

- Dilute suspensions of Newtonian fluids
- Small droplet deformation
- Includes time-dependent effects
- Thin interface and constant α

$$\eta^* = \mu_m \left[\frac{1 + 3\phi H^*(\omega)}{1 - 2\phi H^*(\omega)} \right]$$

13

Oldroyd's emulsion model (1953,1955)

- $H^*(\omega)$ operator:

$$H^*(\omega) = \frac{A + Bi\omega}{C + Di\omega} = \frac{AC + i\omega (BC - AD) + \omega^2 BD}{C^2 + D^2\omega^2}$$

$$A = \frac{8\alpha}{d_p} (2 + 5k)$$

$$B = \mu_m (k - 1)(16 + 19k)$$

$$C = \frac{80\alpha}{d_p} (1 + k)$$

$$D = \mu_m (3 + 2k)(16 + 19k)$$

14

Example 8.2-1

- Predict LVE behavior by Oldroyd emulsion model
- Expansion of previous equation → retaining only the linear term in ϕ (dilute suspensions)

$$\begin{aligned}\eta^* &= \mu_m (1 + 5\phi H^*) \\ &= \mu_m \left[1 + 5\phi \frac{AC + BD\omega^2}{C^2 + D^2\omega^2} \right] + i\omega 5\phi \mu_m \frac{BC - AD}{C^2 + D^2\omega^2}\end{aligned}$$

15

Example 8.2-1

$$\eta' = \frac{G''}{\omega} = \mu_m \left[1 + 5\phi \frac{AC + BD\omega^2}{C^2 + D^2\omega^2} \right]$$

$$\eta'' = \frac{G'}{\omega} = 5\omega\phi\mu_m \frac{AD - BC}{C^2 + D^2\omega^2}$$

At low frequencies: $G' \propto \omega^2$

$G'' \propto \omega$

$$\lim_{\omega \rightarrow 0} \eta^* = \eta_0 = \mu_m \left[1 + 5\phi \frac{A}{C} \right] = \mu_m \left[1 + \frac{2 + 5k}{2(1+k)} \phi \right]$$

Taylor result

16

Example 8.2-1

- Terminal relaxation time of the emulsion:

$$\lambda_0 = \lim_{\omega \rightarrow 0} \frac{G'}{\eta' \omega^2} = \frac{\frac{\mu_m \phi}{160(\alpha/d_p)} \left[\frac{16 + 19k}{1+k} \right]^2}{1 + \frac{2 + 5k}{2(1+k)} \phi}$$

- At low frequencies \rightarrow behavior of a viscoelastic fluid
- Terminal time \propto concentration of droplets and to d_p/α

17

Palierne model (1990)

- Most interesting extension of the Oldroyd emulsion model
- LVE behavior of non-dilute suspensions of viscoelastic droplets in a viscoelastic matrix
- Dipole-type interactions included
- Droplet size and size distribution included

18

Palierne model (1990)

- Description of the suspension complex modulus:

$$G_s^*(\omega) = G_m^*(\omega) \frac{1 + 3 \sum_i \phi_i H_i^*(\omega)}{1 - 2 \sum_i \phi_i H_i^*(\omega)}$$

$$H_i^*(\omega) = \frac{8(\alpha/d_i) [2G_m^*(\omega) + 5G_d^*(\omega)] + [G_d^*(\omega) - G_m^*(\omega)] [16G_m^*(\omega) + 19G_d^*(\omega)]}{80(\alpha/d_i) [G_m^*(\omega) + G_d^*(\omega)] + [2G_d^*(\omega) + 3G_m^*(\omega)] [16G_m^*(\omega) + 19G_d^*(\omega)]}$$

- ϕ_i = volume fraction of droplet with diameter d_i
- No empirical parameters

19

Simplified Palierne model

- Assumption \rightarrow monodisperse size using volume average diameter d_v (representative of size distribution)

$$G'_s = \frac{1}{D} [G'_m (B_1 B_2 + B_3 B_4) - G''_m (B_4 B_1 - B_2 B_3)]$$

$$G''_s = \frac{1}{D} [G'_m (B_4 B_1 - B_2 B_3) - G''_m (B_1 B_2 + B_3 B_4)]$$

$$B_1 = C_1 - 2\phi C_3$$

$$B_2 = C_1 + 3\phi C_3$$

$$B_3 = C_2 - 2\phi C_4$$

$$B_4 = C_2 + 3\phi C_4$$

$$D = (C_2 - 2\phi C_4)^2 + (C_1 - 2\phi C_3)^2$$

20

Simplified Palierne model

- With:

$$C_1 = 80 \frac{\alpha}{d_v} (G'_m + G'_d) + 38(G_d'^2 - G_d''^2) + 48(G_m'^2 - G_m''^2) + 89(G'_m G'_d - G''_m G''_d)$$

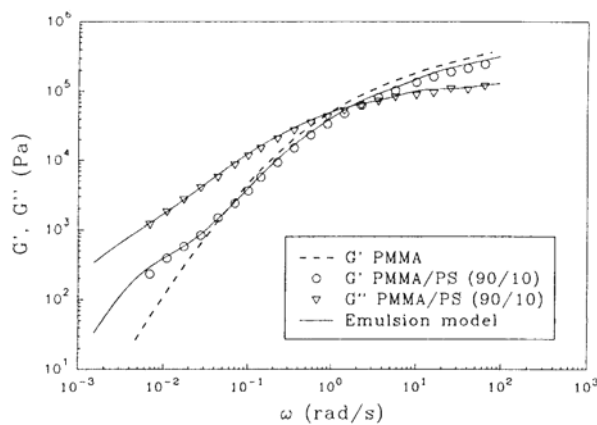
$$C_2 = 80 \frac{\alpha}{d_v} (G''_m + G''_d) + 96 G'_m G''_m + 76 G'_d G''_d + 89 (G''_m G'_d + G'_m G''_d)$$

$$C_3 = 8 \frac{\alpha}{d_v} (2G'_m + 5G'_d) - 16(G_m'^2 - G_m''^2) + 19(G_d'^2 - G_d''^2) - 3(G'_m G'_d - G''_m G''_d)$$

$$C_4 = 8 \frac{\alpha}{d_v} (2G''_m + 5G''_d) - 32G'_m G''_m + 38G'_d G''_d - 3(G''_m G'_d + G'_m G''_d)$$

21

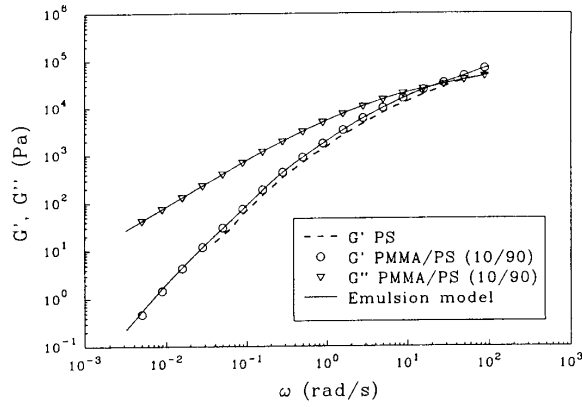
Palierne model applied to polymer blends



90/10% PMMA/PS
(Carreau et al., 1994)

22

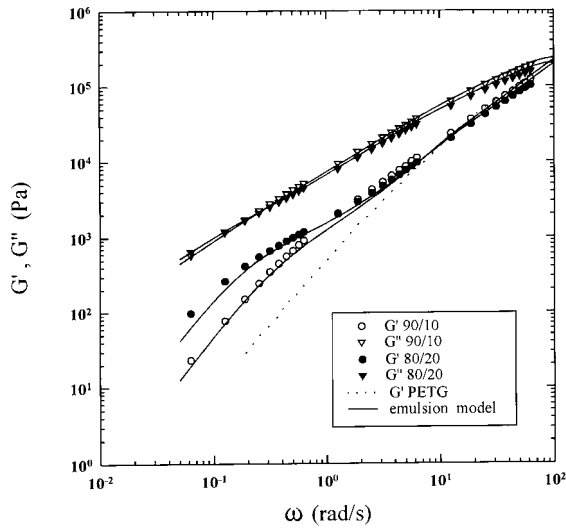
Palierne model applied to polymer blends



10/90% PMMA/PS
(Carreau et al., 1994)

23

Palierne model applied to polymer blends



Blend	α (mN/m)
90/10% PETG/EVA	3.9
80/20% PETG/EVA	4.5

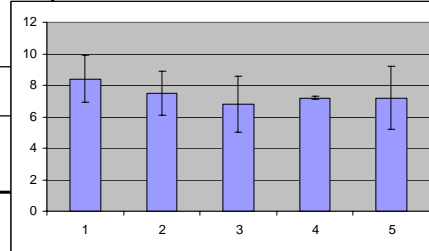
(Lacroix et al., 1996)

24

Estimate of interfacial tension

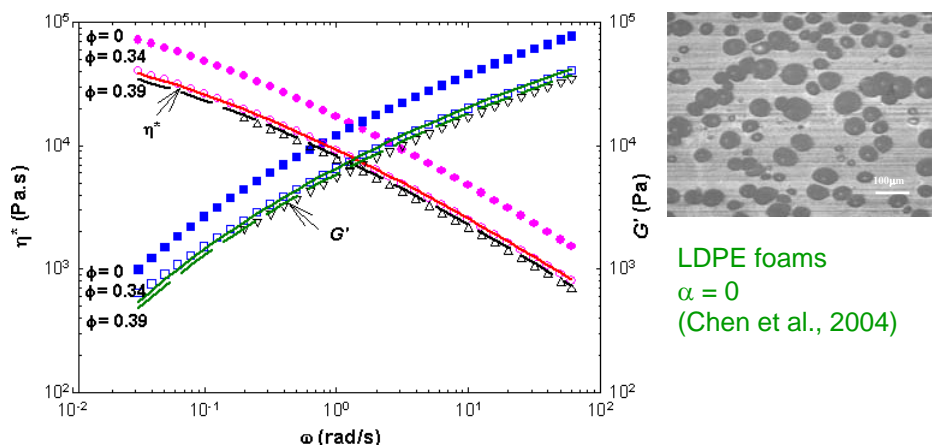
Method	Interfacial tension (mN/m)
1) Breaking thread	8.4 ± 1.5
2) Imbedded fiber retraction	7.5 ± 1.4
3) Retraction of deformed drop	6.8 ± 1.8
4) Pendant drop	7.2 ± 0.1
5) Palierne model	7.2 ± 2.0

PS / nylon 6
(Xing et al., 2000)



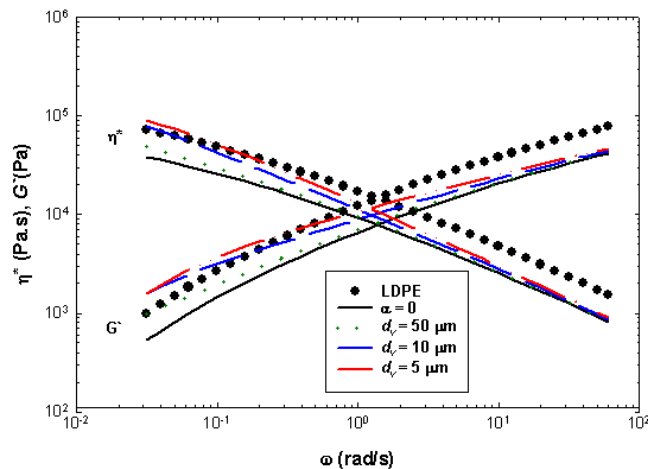
25

Palierne model applied to polymer foams



26

Palierne model applied to polymer foams



LDPE foams
Surface tension:
 $\alpha = 27 \text{ mN/m}$

(Chen et al., 2004)

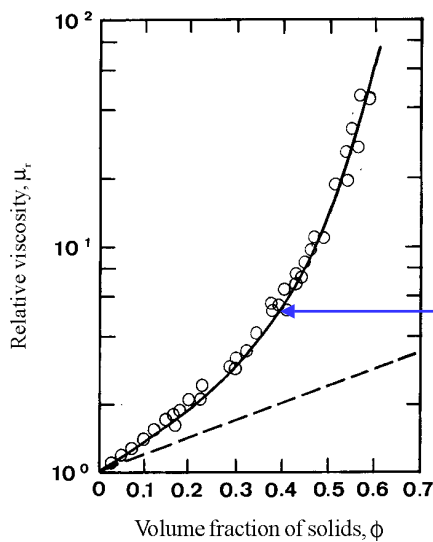
27

Palierne model: Summary

- Good agreement with experimental results of viscoelastic emulsions
- Can be used to obtain an estimate of the interfacial tension
- Applicable to polymer foams
- Fail in the case of strong particle-particle interactions or agglomerated particles

28

Concentrated suspensions of non-interactive particles



Suspensions of spheres of low interaction in a Newtonian fluid (Thomas 1965)

$$\mu_r = \frac{\mu_s}{\mu_m} = \left[1 + \frac{\phi}{\phi_m} \right]^{-2}$$

Maron-Pierce equation

29

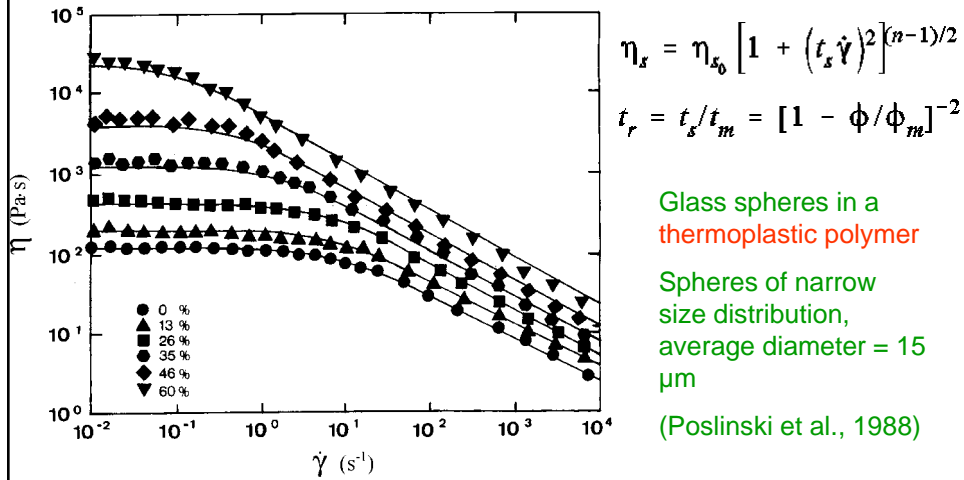
Concentrated suspensions of non-interactive particles

- **Non-Newtonian behavior** of polymer filled with non-interactive spheres is very similar to that of non-filled polymers, up to a solid fraction close to maximum packing
- Possible description of the viscosity by the Carreau (1972) equation:

$$\eta_x = \eta_{s_0} \left[1 + (\dot{\gamma}_x \dot{\gamma})^2 \right]^{(n-1)/2}$$

30

Concentrated suspensions of non-interactive particles



31

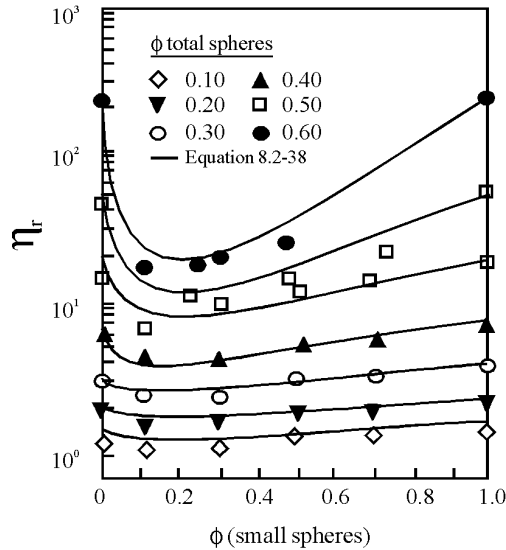
Concentrated suspensions of non-interactive particles

- Large increase of the time constant with solid content \rightarrow increase of non-Newtonian effects
- Poslinski (1988) also proposed using **Maron-Pierce equation** for non-Newtonian systems if viscosity values are compared at the same stress:

$$\eta_r = (\eta_s / \eta_m) \Big|_{\sigma_{12}} = [1 - \phi / \phi_m]^{-2}$$

32

Effect of polydisperse spheres



Glass beads in a polybutene @ 22°C
(small spheres ~ 15 μ m, large spheres ~ 78 μ m) (Poslinski et al., 1988)

→ Polydispersity reduces suspension viscosity

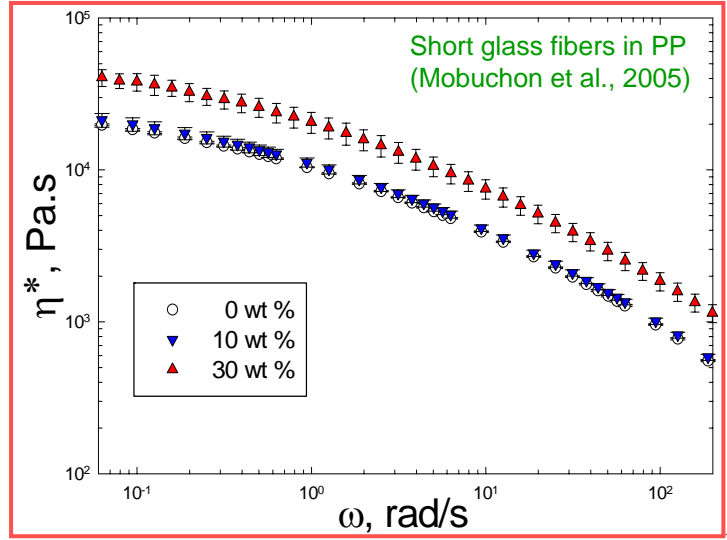
33

Elasticity of suspensions of spheres

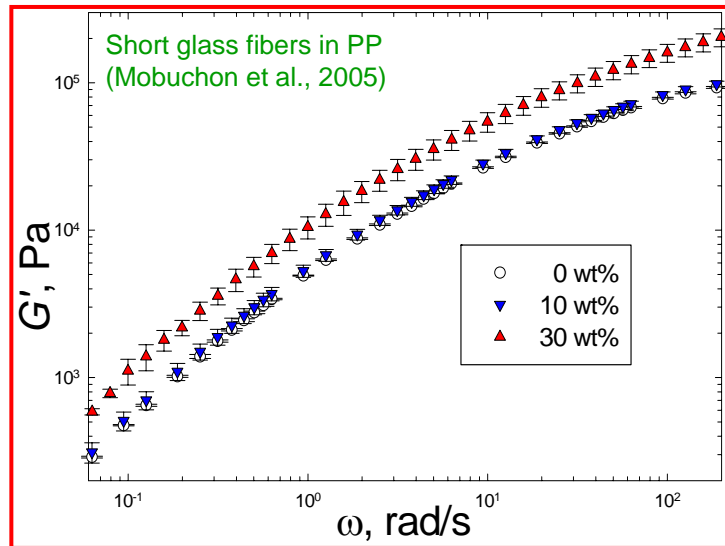
- Limited data available
- Contradictory
- Faulkner and Schmidt (1977) → G'' increases more rapidly than G'
- Poslinski et al. (1988) → G' increases more rapidly than G''
- ...

34

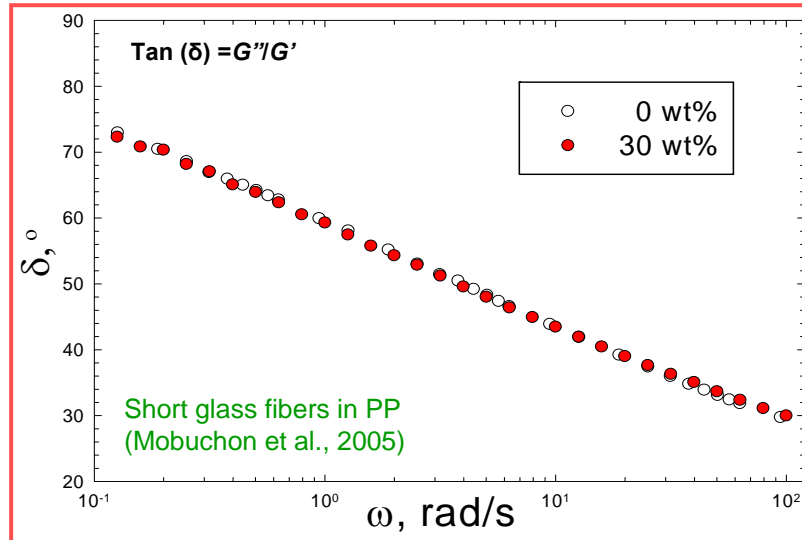
Complex viscosity: fiber-filled system



Elastic moduli: fiber-filled system



Loss angle: fiber-filled system

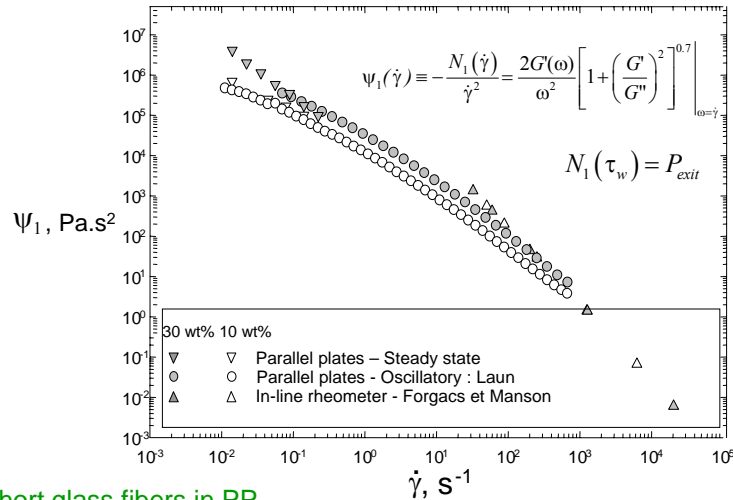


Palierne model

For the particular case, $G_1^* \gg G_M^*$, the Palierne model yields the following expression:

$$G_B^* = \left(\frac{1 + 3/2\phi}{1 - \phi} \right) G_M^* \quad \Rightarrow \quad \tan \delta_B = \tan \delta_M$$

First normal stress coefficient



Short glass fibers in PP
(Mobuchon et al., 2005)

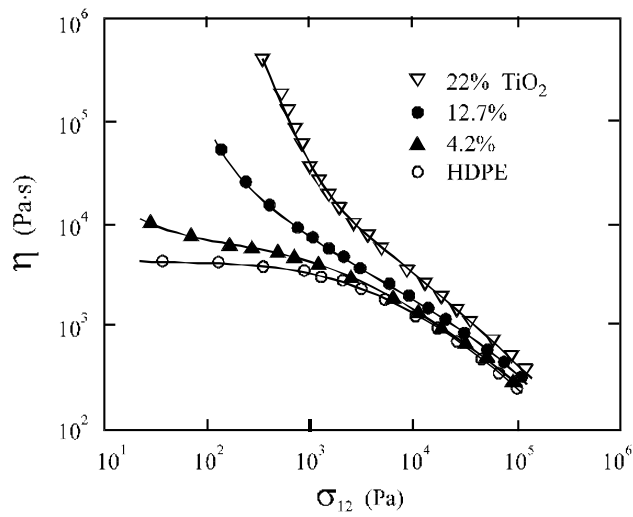
39

Concentrated suspensions of interactive particles

- Complications arise when interparticle interactions are larger than viscous forces
 - Agglomeration of particles → viscosity increase, mainly at low shear rates
 - For highly concentrated suspensions → yield stress
 - Viscosity highly dependent on interfacial properties and sizes of particles aggregates
 - Blending conditions are critical

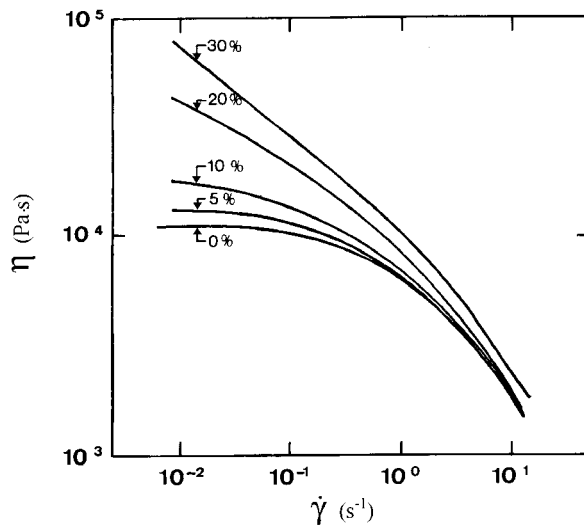
40

Rutile (TiO₂) particles in HDPE



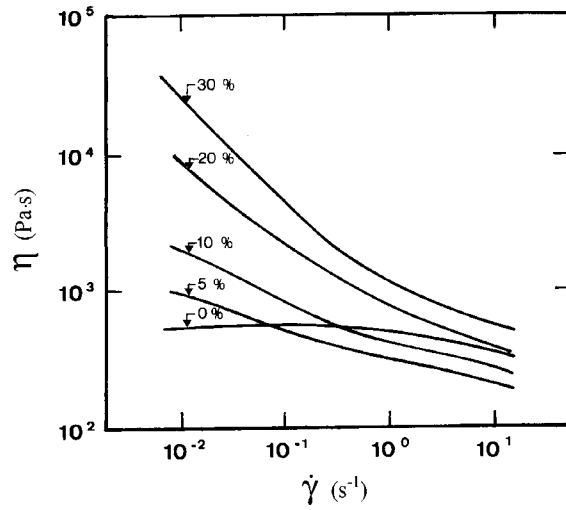
41

Carbon black particles in PS



42

Carbon black particles in PS



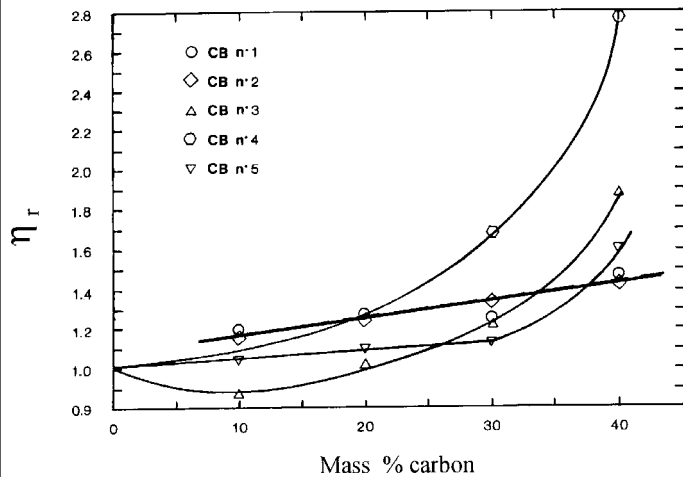
230°C - Solid content
in mass %

Viscosity gets smaller
than matrix at low
solid content →
possible reduction of
entanglements in the
presence of solid
particles... or polymer
degradation at high T°

Lakdawala & Salovey
(1987)

43

Carbon black particles in HDPE



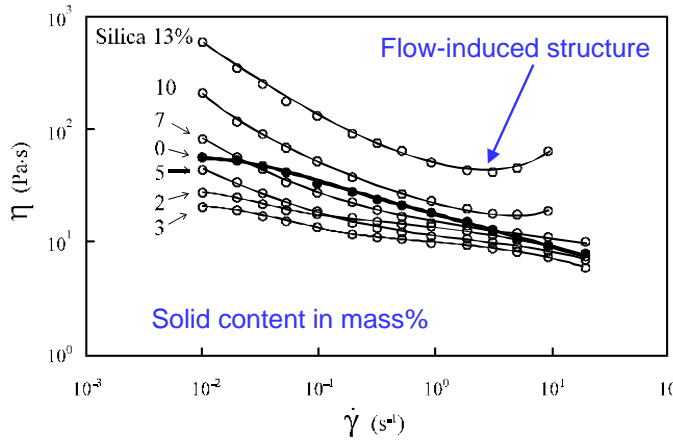
Shear rate = 10 s⁻¹

Five different
types of carbon
black → viscosity
dependent on
surface properties

Dufresne (1989)

44

Suspensions of fumed silica particles

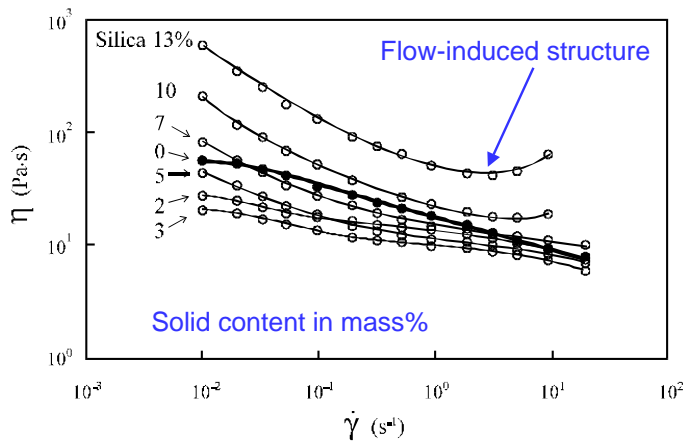


Polyacrylamide (PAA) in glycerine (Otsubo (1986))

Hydroxyl groups at the surface of fumed silica particles favor adsorption of PAA chains → reduction of the viscosity at low solid content

45

Suspensions of fumed silica particles

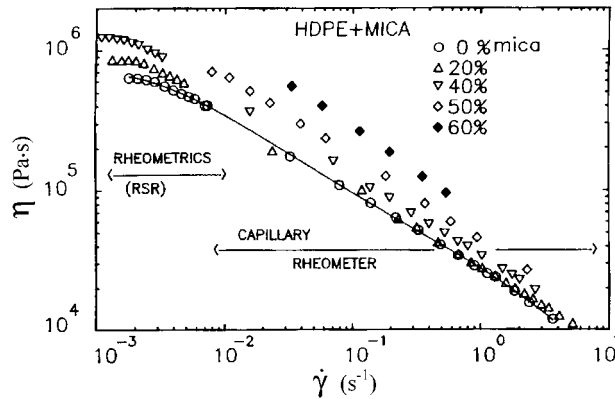


Polyacrylamide (PAA) in glycerine (Otsubo (1986))

Complex behavior at high solid content

46

HDPE filled with mica



220°C - Solid content in mass %

Alignment and orientation of mica flakes → slight viscosity increase (much smaller than with carbon black)

Malik et al. (1988)

47

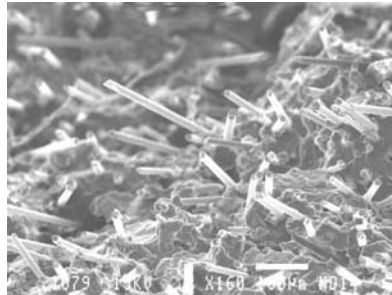
Short-fiber filled polymers

Thermoplastics reinforced by short fibers:

- Industrial materials
- Complex behavior in molten state

Applications:

- Glass mat reinforced thermoplastics
- Extrusion
- Injection
- Thermoforming

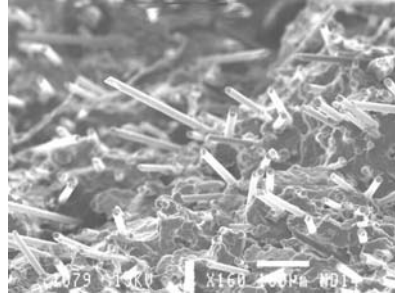


48

Short-fiber filled polymers

Computational and experimental results from:

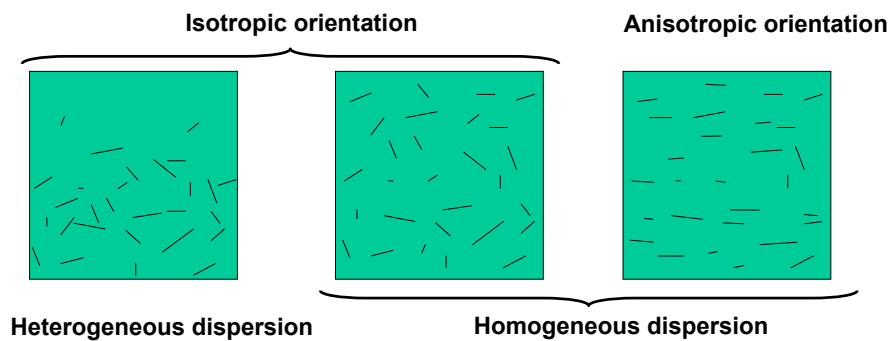
- Maryam Sepehr
- Christophe Mobuchon
- Julien Ferec



49

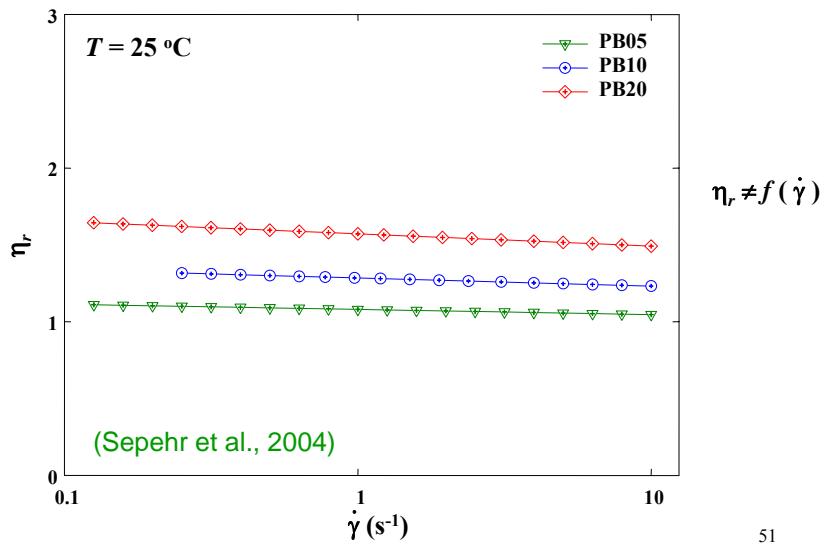
Microstructure

Macrocomposite thermoplastic/rigid fibers



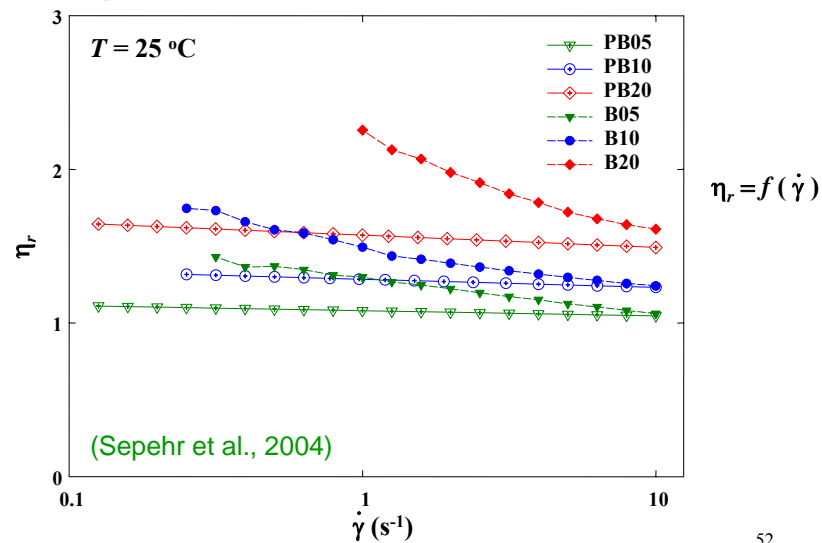
50

Reduced viscosity of a fiber-filled Newtonian fluid (polybutene)



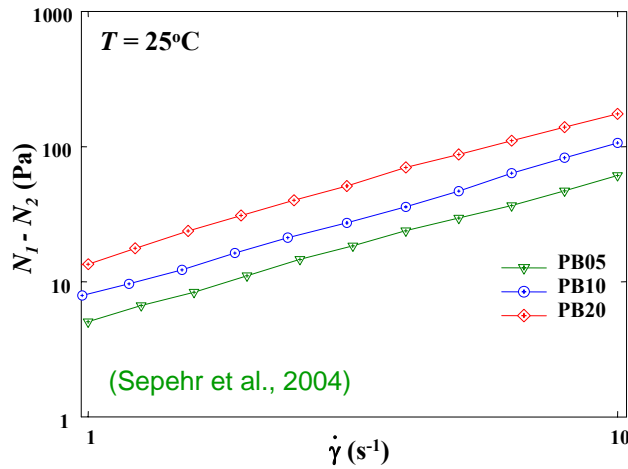
51

Reduced viscosity of a fiber-filled Boger fluid (PB+PIB+kerosene)



52

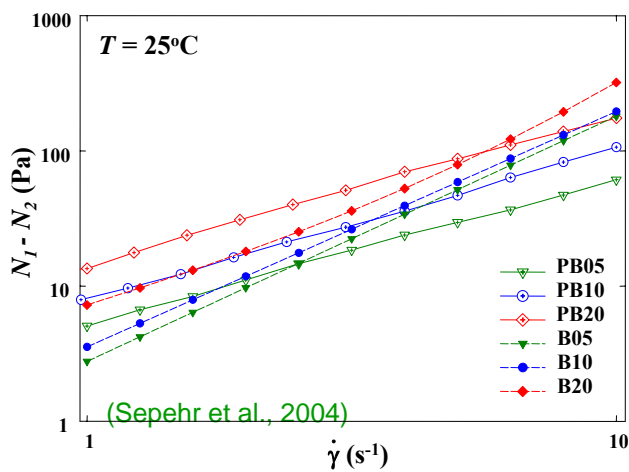
Normal stress difference of a fiber-filled Newtonian fluid (polybutene)



$N_1 - N_2$ is a **linear** function of the shear rate

53

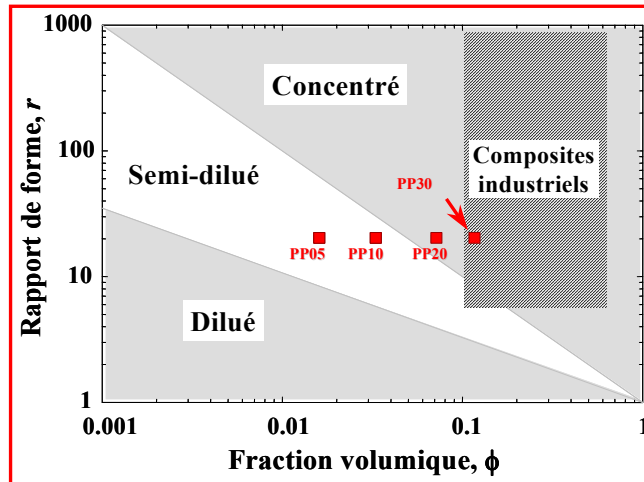
Normal stress difference of a fiber-filled Boger fluid (PB+PIB+kerosene)



$N_1 - N_2$ is a **quadratic** function of the shear rate

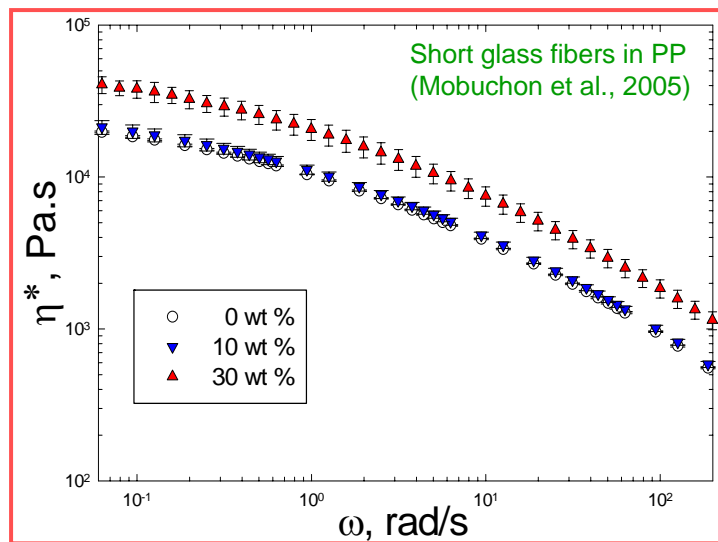
54

Concentration regimes of fiber-filled polymers



55

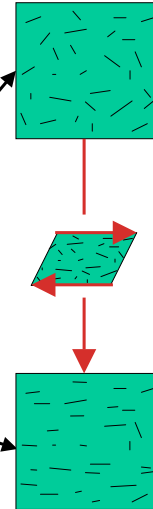
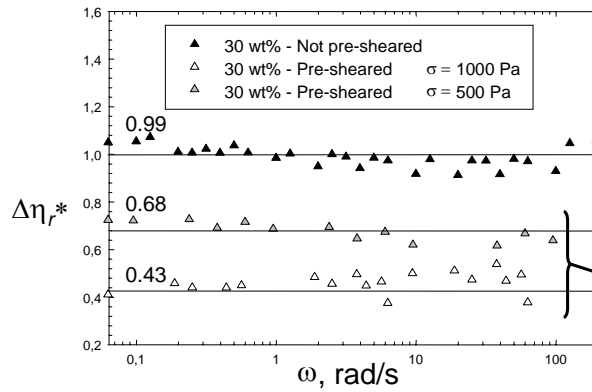
Complex viscosity



56

Effect of orientation

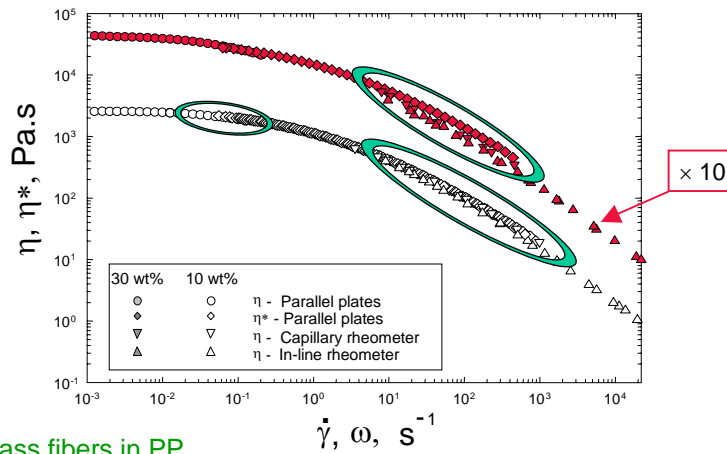
$$\Delta\eta_r^*(\omega) = \frac{\eta_{suspension}^* - \eta_{matrix}^*}{\eta_{matrix}^*} \Big|_{\omega}$$



Short glass fibers in PP
(Mobuchon et al., 2005)

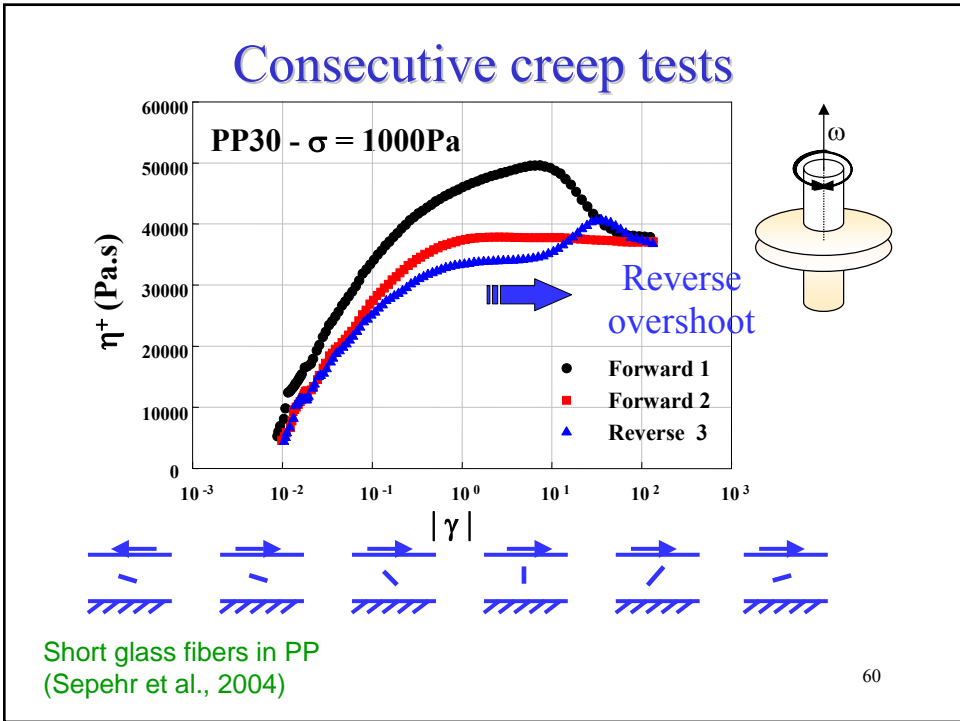
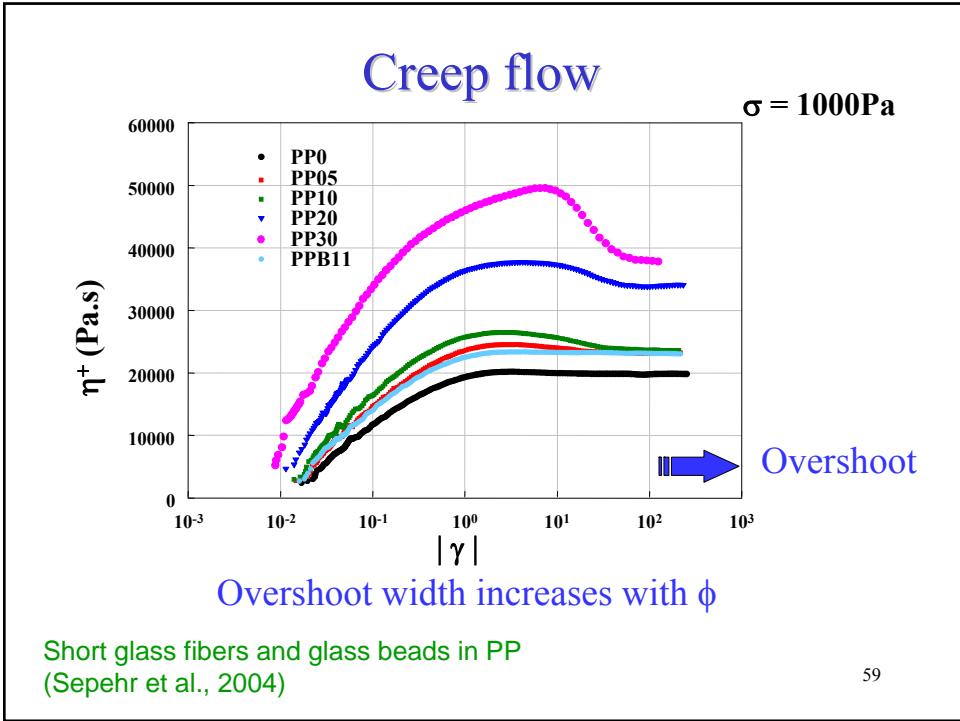
57

High shear rate measurements

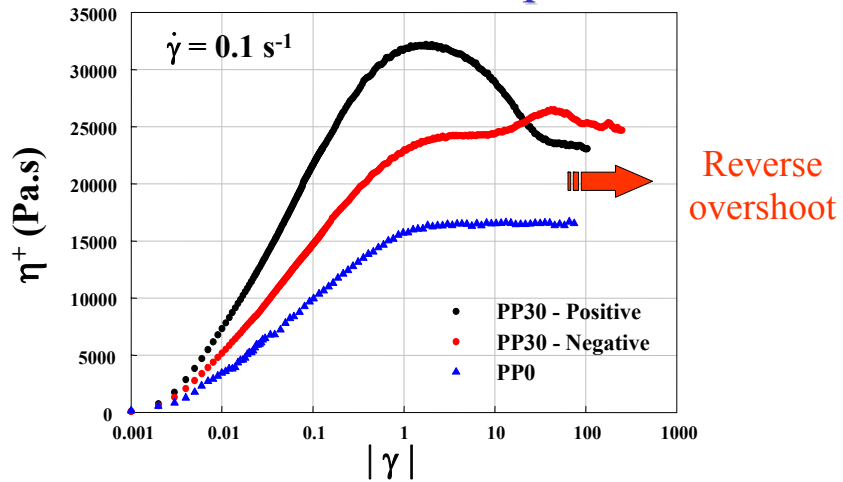


Short glass fibers in PP
(Mobuchon et al., 2005)

58



Consecutive start-up tests

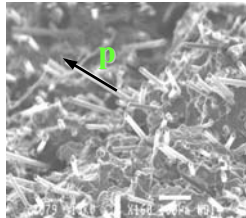


Reverse overshoot for PP30 in start-up test

Short glass fibers in PP
(Sepehr et al., 2004)

61

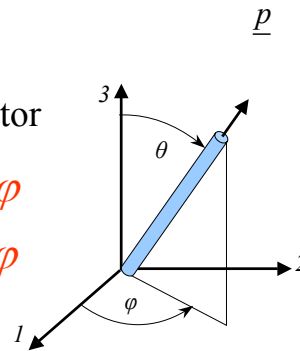
Single fiber orientation



Single fiber:

• $\underline{p}(\varphi, \theta)$: unit vector

$$\underline{p} \begin{cases} p_1 = \sin \theta \cos \varphi \\ p_2 = \sin \theta \sin \varphi \\ p_3 = \cos \theta \end{cases}$$



62

Multiple fiber orientation

Multiple fibers:

- $\psi(\underline{p})$: statistical orientation distribution function
 $P(\theta_1 \leq \theta \leq \theta_1 + d\theta, \phi_1 \leq \phi \leq \phi_1 + d\phi) = \Psi(\theta_1, \phi_1) \sin\theta_1 d\theta d\phi$
- Even function
- Convected quantity: $\frac{D\Psi}{Dt} = -\frac{\partial}{\partial \underline{p}} \cdot (\Psi \underline{\dot{p}})$
- Orientation distribution function calculation \rightarrow requires very large computational efforts

63

Multiple fiber orientation

Fokker-Planck equation $\frac{d\Psi}{dt} = -\underbrace{\frac{\partial}{\partial p_i} (\Psi \dot{p}_i)}_{\text{Convection term}} + D_r \underbrace{\frac{\partial^2 \Psi}{\partial p_i^2}}_{\text{Diffusion term}}$

Jeffery (1922)

D_r : Diffusion coefficient

Model	Material parameters
Jeffery (1922)	$D_r = 0, \lambda = \frac{r^2 - 1}{r^2 + 1}$
Dinh & Armstrong (1984)	$D_r = 0, \lambda = 1$
Folgar & Tucker (1984)	$D_r = C_I \dot{\gamma}, \lambda = 1$
Kamal & Mutel (1989)	$D_r = \text{cte}, \lambda = \frac{r^2 - 1}{r^2 + 1}$

C_I : Interaction coefficient (empirical)

64

Multiple fiber orientation

- a_2 and a_4 : 2nd and 4th order orientation tensors
- Dyadic products of \mathbf{p} averaged over orientation space
- More compact and efficient description

$$a_{ij} = a_2 = \oint p_i p_j \psi(\mathbf{p}) d\mathbf{p}$$

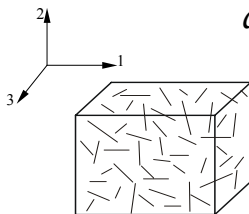
$$a_{ijkl} = a_4 = \oint p_i p_j p_k p_l \psi(\mathbf{p}) d\mathbf{p}$$

65

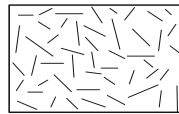
Multiple fiber orientation

$$a_{ij} = a_2 = \oint p_i p_j \psi(\mathbf{p}) d\mathbf{p}$$

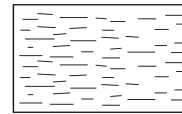
$$a_{ijkl} = a_4 = \oint p_i p_j p_k p_l \psi(\mathbf{p}) d\mathbf{p}$$



$$a_{ij} = \begin{bmatrix} 1/3 & 0 & 0 \\ 0 & 1/3 & 0 \\ 0 & 0 & 1/3 \end{bmatrix}$$



$$a_{ij} = \begin{bmatrix} 1/2 & 0 & 0 \\ 0 & 1/2 & 0 \\ 0 & 0 & 0 \end{bmatrix}$$

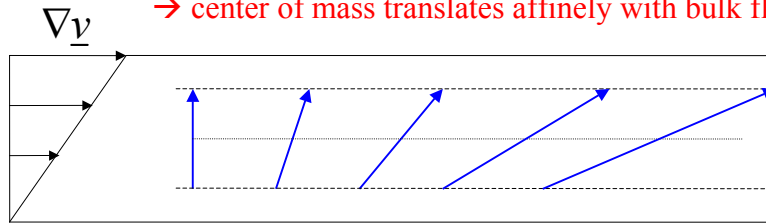


$$a_{ij} = \begin{bmatrix} 1 & 0 & 0 \\ 0 & 0 & 0 \\ 0 & 0 & 0 \end{bmatrix}$$

66

Orientation dynamics

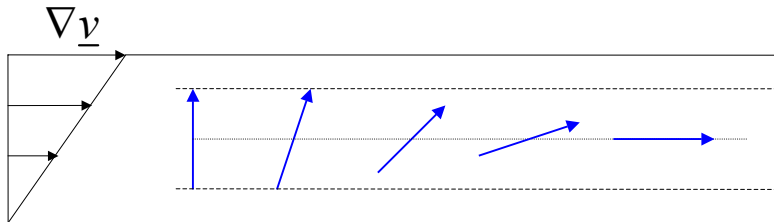
- Single fiber → rigid particle in infinite Newtonian liquid
 → external and inertia forces neglected
 → center of mass translates affinely with bulk flow



$$\frac{d\underline{p}}{dt} = \dot{\underline{p}} = \nabla \underline{v} \cdot \underline{p} \quad \nabla \underline{v} = \begin{bmatrix} 0 & 0 & 0 \\ \dot{\gamma} & 0 & 0 \\ 0 & 0 & 0 \end{bmatrix}$$

67

Orientation dynamics

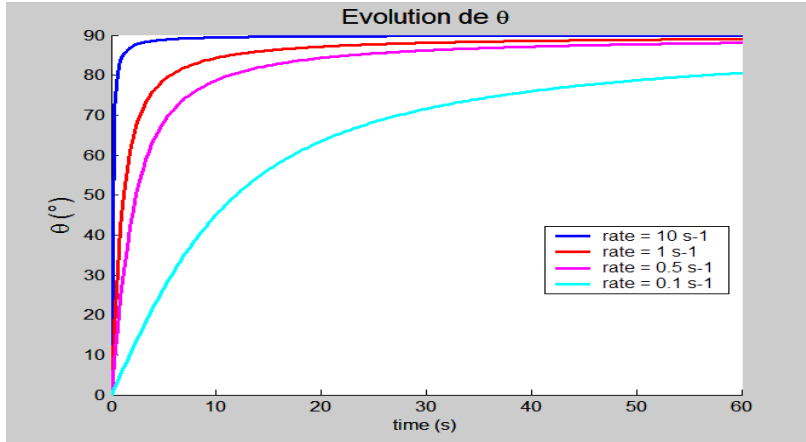


$$\dot{\underline{p}} = \nabla \underline{v} \cdot \underline{p} - \nabla \underline{v} \cdot \underline{p} \underline{p} \underline{p}$$

- Stretching part of motion is subtracted off
 → Conservation of vector \underline{p} unit norm

68

Orientation dynamics

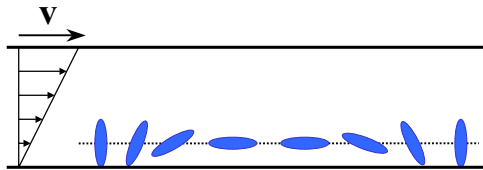


(J. Ferec)

69

Orientation dynamics

$$\dot{\underline{p}} = -\frac{1}{2}\underline{\omega} \cdot \underline{p} + \frac{1}{2}\lambda \left(\underline{\dot{\gamma}} \cdot \underline{p} - \underline{\dot{\gamma}} : \underline{p} \underline{p} \underline{p} \right) \quad \text{Jeffery (1922)}$$

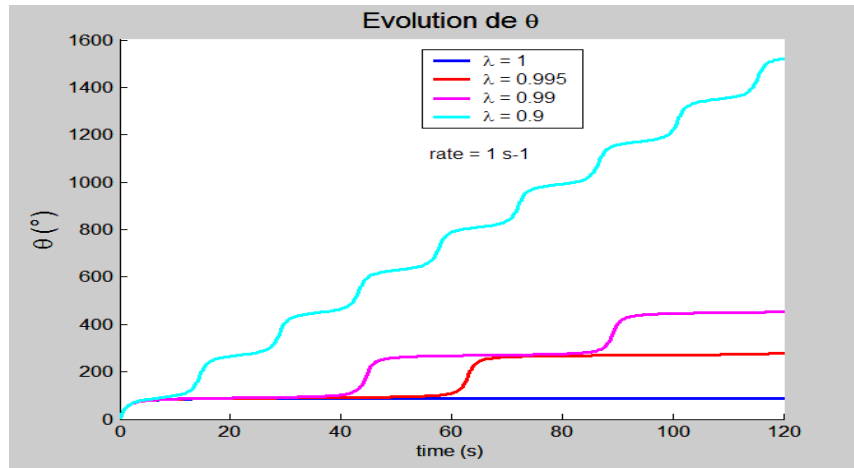


closed periodic rotation according to Jeffery orbital in simple shear

with $\underline{\dot{\gamma}} = (\nabla \underline{v}^T + \nabla \underline{v})$ and $\underline{\omega} = (\nabla \underline{v}^T - \nabla \underline{v})$ and $\lambda = \frac{r^2 - 1}{r^2 + 1}$
 r : fibers shape factor (L/D)

70

Orientation dynamics



(J. Ferec)

71

Multiple fibers

$$\frac{Da_{ij}}{Dt} = \underbrace{-\frac{1}{2}(\omega_{ik}a_{kj} - a_{ik}\omega_{kj}) + \frac{1}{2}\lambda(\dot{\gamma}_{ik}a_{kj} + a_{ik}\dot{\gamma}_{kj} - 2\dot{\gamma}_{kl}a_{ijkl})}_{\text{Convective term}}$$

Convective term

$$+ \underbrace{2D_r(\delta_{ij} - 3a_{ij})}_{\text{Isotropic rotation diffusion term}}$$

Isotropic rotation diffusion term

$$D_r = C_I \overline{\dot{\gamma}}$$

C_I : Interaction coefficient (semi-dilute systems)

$\overline{\dot{\gamma}}$: Rate of deformation tensor amplitude

$a_{ijkl} = f(a_{ij})$: closure approximation

Folgar and Tucker (1984)

72

Multiple fibers

$$\frac{Da_{ij}}{Dt} = \underbrace{-\frac{1}{2}(\omega_{ik}a_{kj} - a_{ik}\omega_{kj}) + \frac{1}{2}\lambda(\dot{\gamma}_{ik}a_{kj} + a_{ik}\dot{\gamma}_{kj} - 2\dot{\gamma}_{kl}a_{ijkl})}_{\text{Convective term}} + \underbrace{2D_r(\delta_{ij} - 3a_{ij})}_{\text{Isotropic rotation diffusion term}}$$

$$D_r = C_I \bar{\dot{\gamma}}$$

Model	Interaction coefficient
Bay (1991)	$C_I = 0.0184 \exp(-0.7148\phi r)$
Ranganathan et Advani (1991)	$C_I = \frac{C_I^*}{(h/L)}$
Phan-Thien <i>et al.</i> (2002)	$C_I = A[1 - \exp(-B\phi r)]$

73

Closure approximations

Linear

$$\hat{a}_{ijkl} = -\frac{1}{35}(\delta_{ij}\delta_{kl} + \delta_{ik}\delta_{jl} + \delta_{il}\delta_{jk}) + \frac{1}{7}(a_{ij}\delta_{kl} + a_{ik}\delta_{jl} + a_{il}\delta_{jk} + a_{kl}\delta_{ij} + a_{jl}\delta_{ik} + a_{jk}\delta_{il})$$

Quadratic

$$\tilde{a}_{ijkl} = a_{ij}a_{kl}$$

Hybrid

$$\bar{a}_{ijkl} = (1-f)\hat{a}_{ijkl} + f\tilde{a}_{ijkl}$$

Advani (1987)

$$f = 1 - 27 \det[a_{ij}]$$

Orthotropic and Natural

Cintra et Tucker (1995)

74

Constitutive equation

$$\boldsymbol{\sigma} = \underbrace{\eta_m \dot{\boldsymbol{\gamma}}}_{\text{Matrix contribution}} + \eta_m \phi \underbrace{\left\{ \mu_1 \dot{\boldsymbol{\gamma}} + \mu_2 \dot{\boldsymbol{\gamma}} : \mathbf{a}_4 + \mu_3 [\dot{\boldsymbol{\gamma}} \cdot \mathbf{a}_2 + \mathbf{a}_2 \cdot \dot{\boldsymbol{\gamma}}] + 2\mu_4 \mathbf{a}_2 D_r \right\}}_{\text{Axisymmetric particles contribution}}$$

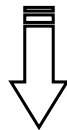
η_m : Matrix viscosity
 ϕ : Fibers volume fraction Tucker et Advani (1994)
 μ_i : Material parameters

Models	Material Parameters
Hinch et Leal (1972)	$\mu_1 = 2, \mu_2 = \frac{r^2}{2[\ln(2r) - 1.5]}, \mu_3 = \frac{6 \ln 2r - 11}{r^2}, \mu_4 = 0.$
Lipscomb (1987)	$\mu_1 = 2, \mu_2 = \frac{r^2}{2 \ln(r)}, \mu_3 = \mu_4 = 0.$
Shaqfeh et Fredrickson (1990)	$\mu_2 = \frac{16r^2}{3 \ln(1/\phi)} \left[1 - \frac{\ln \ln(1/\phi)}{\ln(1/\phi)} + \frac{0.6634}{\ln(1/\phi)} \right], \mu_1 = \mu_3 = \mu_4 = 0.$

Model for dilute and semi-dilute suspensions

System of coupled equations

$$\begin{cases} \dot{\mathbf{a}}_2 = f(\mathbf{a}_2, \mathbf{a}_4, \nabla \mathbf{v}) \\ \mathbf{a}_4 = g(\mathbf{a}_2) \\ \boldsymbol{\sigma} = h(\mathbf{a}_2, g(\mathbf{a}_2), \nabla \mathbf{v}) \end{cases}$$



Modèle pour suspensions concentrées

FTL model

FTL model : Folgar-Tucker-Lipscomb

Orientation evolution equation:

$$\frac{Da_{ij}}{Dt} = -\frac{1}{2}(\omega_{ik}a_{kj} - a_{ik}\omega_{kj}) + \frac{1}{2}\lambda(\dot{\gamma}_{ik}a_{kj} + a_{ik}\dot{\gamma}_{kj} - 2\dot{\gamma}_{kl}a_{ijkl}) + 2C_I\bar{\dot{\gamma}}(\delta_{ij} - 3a_{ij})$$

Constitutive equation:

$$\sigma_{ij} = \eta_m \dot{\gamma}_{ij} + \eta_m \phi \left\{ 2\dot{\gamma}_{ij} + \mu_2 \dot{\gamma}_{kl} : a_{ijkl} \right\}$$

$$\mu_2 = \frac{r^2}{2 \ln(r)}$$

77

Simple shear flow

Rheological functions from FTL model :

$$\begin{aligned} \eta = \frac{\sigma_{12}}{\dot{\gamma}} &= \eta_m [1 + 2\phi(1 + \mu_2 a_{1212})] \\ N_1 = \sigma_{11} - \sigma_{22} &= 2\eta_m \mu_2 \phi \dot{\gamma} (a_{1112} - a_{2212}) \\ N_2 = \sigma_{22} - \sigma_{33} &= 2\eta_m \mu_2 \phi \dot{\gamma} (a_{2212} - a_{3312}) \end{aligned} \quad \left\{ \begin{array}{l} \mathbf{a}_2 = f(\mathbf{a}_2, \mathbf{a}_4, \nabla \mathbf{v}) \\ \mathbf{a}_4 = g(\mathbf{a}_2) \\ \sigma = h(\mathbf{a}_2, \mathbf{a}_4, \nabla \mathbf{v}) \end{array} \right.$$

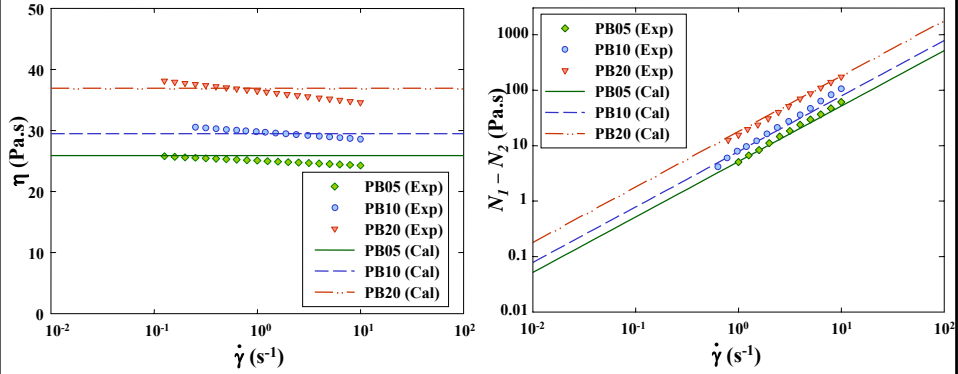
Lipscomb et al. (1988)

Adjustable parameters:

- C_I Fiber-fiber interaction parameter
- μ_2 Geometric shape factor coefficient

78

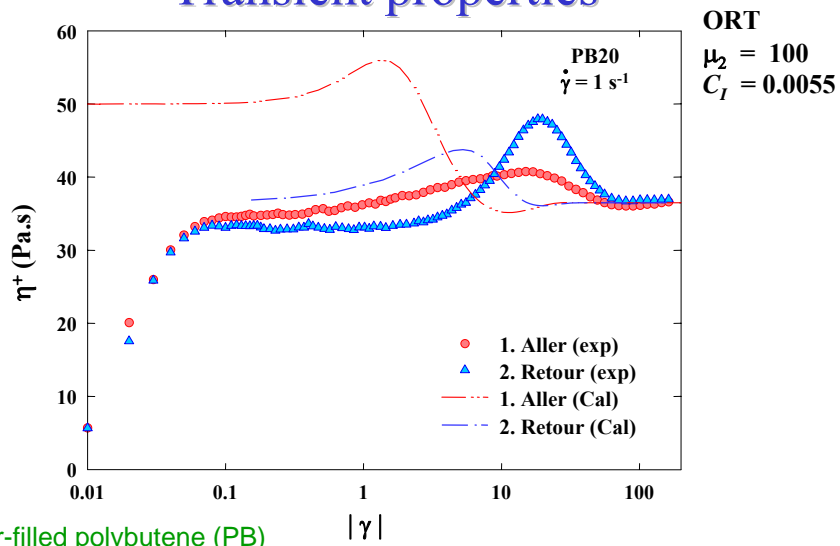
Steady-state properties



Fiber-filled polybutene (PB)
Sepehr et al., 2004

79

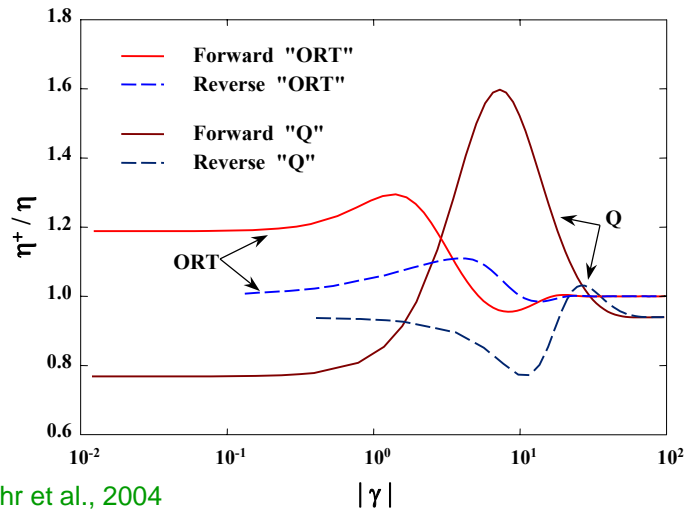
Transient properties



Fiber-filled polybutene (PB)
Sepehr et al., 2004

80

Closure approximations effects



81

Modified FTL model

Introduction of a “slip” factor:

$$\gamma_s = \alpha \dot{\gamma} t \quad \begin{array}{l} \gamma_s : \text{Deformation} \\ \alpha : \text{Slip factor} \end{array}$$

Three key parameters control the model predictions of the viscosity overshoot:

C_1 Reversal overshoot, shape & amplitude

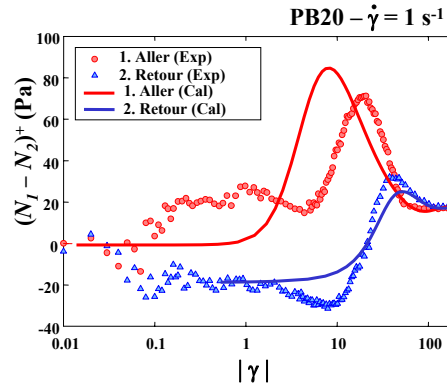
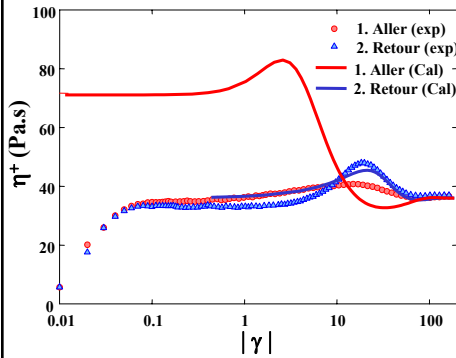
μ_2 Overshoot amplitude

α Overshoot width

82

Modified FTL model

Sepher et al., 2004



ORF

$\mu_2 = 195$
 $C_I = 0.001$
 $\alpha = 0.5$
 $\lambda = 1.0222$

83

Modified FTL model

- Introduction of a slip factor to slow down fiber motion
 → explained by fiber-fiber interactions

But...

- Slip factor can be used only in simple shear
- Model not objective anymore
- Totally phenomenological parameter

84

Summary on fiber-filled polymers

- Adding fibers:
 - $\eta \uparrow$, $\eta^* \uparrow$, $N_1 \uparrow$ but loss angle δ independent of fiber volume fraction
- η^* decreases after pre-shearing due to fiber orientation
- Cox-Merz rule does not apply at high shear rates
- Overshoots \rightarrow fibers orient in the shear plane and flow direction
- Reverse overshoots \rightarrow fibers tilt over when flow direction is reversed
- Reverse overshoots are well controlled and can be used to study particle dynamics

85